



OPEN

# Offshore wind farm operation contributed to a slight improvement in seawater quality along the Jiangsu Coast, China

Zhudeng Wei<sup>1</sup>✉, Minyan Wang<sup>1</sup>, Yang Gao<sup>1</sup>, Wenzheng Yu<sup>1</sup>✉, Aiqing Jia<sup>2</sup>, Zhiyuan You<sup>3</sup> & Zhihong Wang<sup>4</sup>

The rapid growth of offshore wind farms (OWFs) is driven by concerns for energy security and climate change mitigation. However, their impact on marine environments remains poorly understood due to limited research. This study analyzes the effects of an OWF along China's Jiangsu Coast on seawater quality using data from different development phases. Results show the major pollutants were different across phases. Heavy metal pollution reached alert levels during construction compared to the safe levels observed in the pre-construction and operational phases, mainly due to increases in Pb, Cd, and Hg concentrations. Eutrophication was mild throughout all periods but exhibited a continuous decrease, primarily attributed to reductions in PH and COD concentrations. As a result, the comprehensive pollution level during construction was increased, but it was improved to a clean level during the operational phase. Besides, significant variations were observed in the spatial distribution patterns of major pollutant indices across different scenarios. These changes may stem from a combination effect of land-based pollution, aquaculture, OWF-induced disturbances to atmosphere and hydrodynamics, OWF-related drain and leakage contamination, and marine management policies. Understanding these effects informs OWF optimization, rational wind resource utilization, and marine ecology protection.

**Keywords** Offshore wind farm, Surface seawater pollution, Environmental impact assessment, Renewable energy, Jiangsu coastal area

The development of renewable clean energy is driven by energy security and the mitigation of climate change. Wind power has become one of the most important sources of renewable energy globally, with global wind electric capacities growing by 70% between 2015 and 2019<sup>1,2</sup>. The total installed capacity of global wind energy reached 1 TW by the end of 2023, and it is expected to add 680 GW of capacity in the next 5 years<sup>3</sup>. For harnessing wind energy, offshore wind farms (OWFs) possess distinct advantages and greater developmental potential compared to onshore wind farm. For instance, offshore wind is usually stronger and less variable<sup>4</sup>. It witnessed explosive growth of global offshore wind turbines since the twenty-first century<sup>5</sup>. It is evident that OWF will play an increasingly important role in global energy structure transformation and the achievement of carbon emissions reduction and neutrality goals.

With the rise of OWFs, attentions have been drawn to its impact on the marine environment. Numerous studies have noticed and explored the effects of wind farms on species population and structure<sup>6,7</sup>, species migration<sup>8</sup>, marine ecosystem and services<sup>9,10</sup>, marine hydrology<sup>11</sup>, landscape patterns<sup>12</sup>, and the climate environment<sup>13,14</sup>. These impacts are primarily manifested through various factors, including collision risk, habitat destruction, barrier effects, alterations in hydrodynamic and circulation conditions, visual and noise pollution, as well as

<sup>1</sup>School of Geographical Science, Nanjing University of Information Science and Technology, Nanjing 210044, China. <sup>2</sup>China General Nuclear Power Corporation Nantong New Energy Co., Ltd., Nantong 226000, China. <sup>3</sup>Yangzhou City Meteorological Bureau, Yangzhou 225009, China. <sup>4</sup>Three Gorges New Energy Offshore Wind Power Operation and Maintenance Jiangsu Co., Ltd., Yancheng 224100, China. ✉email: weizhudeng@126.com; ywzheng519@126.com

electromagnetic-field effects<sup>14–16</sup>. Regarding the methodology for evaluating the impacts of OWFs, scholars have devised various approaches, spanning from field investigations<sup>17</sup> to ecological modeling<sup>18</sup>, scenario analysis<sup>7</sup>, mathematical statistics<sup>19</sup>, GIS technology<sup>20</sup>, and numerical simulation<sup>13,21</sup>. Additionally, more intricate comprehensive frameworks and conceptual models, such as the DPSIR approach, have been introduced specifically for assessing the environmental impacts of OWFs<sup>15,22</sup>. Nevertheless, researchers acknowledge that the impact of OWFs construction and development on the marine environment is not yet well assessed nor understood<sup>10,14–16</sup>.

Furthermore, it is surprising that only a limited number of studies have focused on the influence of OWFs on seawater quality, which serves as the fundamental environment for marine life and ecosystems. The disruption of seawater quality by OWFs can have far-reaching consequences, impacting not only the marine water environment but also marine biology, sedimentation, fisheries, and maritime transportation. Existing literature reveals that OWFs structures can pose risks to seawater quality, affecting factors ranging from temperature to turbidity, salinity, oxygen levels, and the concentration of nutrients and contaminants<sup>17</sup>. The construction process of OWFs can resuspend seabed sediments, reducing water transparency and adversely affecting marine organisms<sup>12</sup>. Additionally, petroleum contamination and accidental spills during construction and operation can elevate chemical oxygen demand and petroleum concentrations<sup>12</sup>. Corrosion emissions and galvanic anodes may also release chemicals, increasing the concentration of certain metal ions<sup>23</sup>. Given the significance of understanding the effects of OWFs on water quality, it is concerning that many aspects of this impact remain unknown, similar to other aspects of OWFs influence<sup>24</sup>. Some studies suggest that the impact on the marine environment from OWFs may be short-term<sup>15</sup>. Hong et al. have demonstrated a benign water quality during the operation of OWFs in the Pearl River Estuary, China<sup>17</sup>. However, others emphasize the need for quantitative studies to distinguish between positive and negative effects, compare impacts across different development phases, and assess cumulative long-term and large-scale impacts<sup>14</sup>. Achieving these goals necessitates reliance on long-term monitoring data<sup>15,16</sup>. Crucial questions remain unanswered in terms of water quality evaluation: What pollutants do OWFs mainly affect seawater quality? Are there differences in the effects of different pollutants on the seawater quality during construction and subsequent operation? Have the spatial patterns and diffusion mechanisms of pollution changed during different scenarios? Answering these questions will deepen our understanding of environmental pollution distribution and diffusion mechanisms under the influence of OWFs, ultimately supporting the rational development and utilization of wind resources. It is important to note that these patterns may vary depending on situations such as the study area.

This study focuses on a specific OWF located in the Jiangsu coastal area. We developed water quality evaluation indices using data collected from 20 surrounding surface seawater quality monitoring stations. Three scenarios corresponding to pre-construction, construction, and operation phases have been devised to comprehensively assess the impact of the OWF on marine water quality over time, employing mathematical models and GIS technology. We intend to clarify the pollution levels of different types of pollutants, the spatial distribution patterns of pollution, and the dominant ecological risk factors. This study aims to better understand the environmental impact of OWFs development, thereby helping governments or enterprises to take measures for coordinated marine protection and wind energy utilization.

## Data and methods

### Study area

The study area is located in the offshore waters near Rudong County, Jiangsu Province, China (Fig. 1). It boasts favorable geographic conditions and abundant wind energy resources. The coastal terrain is predominantly plains, accounting for over 98.8% of the total area, including the Yellow Sea alluvial plain, the front edge plain of the Yangtze River Delta, and coastal sand spits. The seabed elevation around the OWF ranges from -3.7 to 15.3 m, sloping gradually from west to east. Influenced by the monsoon climate and coastal terrain, current and tidal patterns resulting in complex hydrological conditions<sup>25</sup>.

The central position of the wind farm is approximately 25 km offshore, with a polygonal layout comprising 38 wind turbines. Each turbine has a capacity of 4.0 MW, with a total installed capacity of 152.0 MW. The spacing between turbine rows ranges from 830 to 1360 m, while the spacing between rows is 1060 to 1130 m. The theoretical annual electricity generation of the wind farm is 61,255 million kWh, with an average wake loss coefficient of 6.79%. The large area occupied by the OWF poses a significant threat to the marine environment. Given its proximity to tidal flats, marine aquaculture areas, and marine biodiversity protection zones, changes in water quality within the project area may further affect surrounding ecological environments, which are relatively sensitive.

### Data sources

Around the OWF, a total of 20 surface water quality monitoring stations have been established. These stations are generally parallel to the coastline, distributed in a north-northwest direction (see Fig. 1). Monitoring is conducted once a year in spring. Considering the completeness of the data, this study primarily extracts ten representative water quality parameters, including chemical oxygen demand (COD), petroleum-based pollutants (PET), total inorganic nitrogen (TIN), phosphate (PH), lead (Pb), zinc (Zn), copper (Cu), cadmium (Cd), mercury (Hg), and arsenic (As). Data from pre-construction (2015), construction phase (2016), and operational phase (2018) were meticulously collected and rigorously analyzed to assess the environmental impact of OWF under various scenarios.

### Methodology

Among the methodologies of OWF environmental impacts evaluation, the mathematical models are the most widely used for water quality assessment<sup>19,26,27</sup>, as they provide a macroscopic, comprehensive assessment in

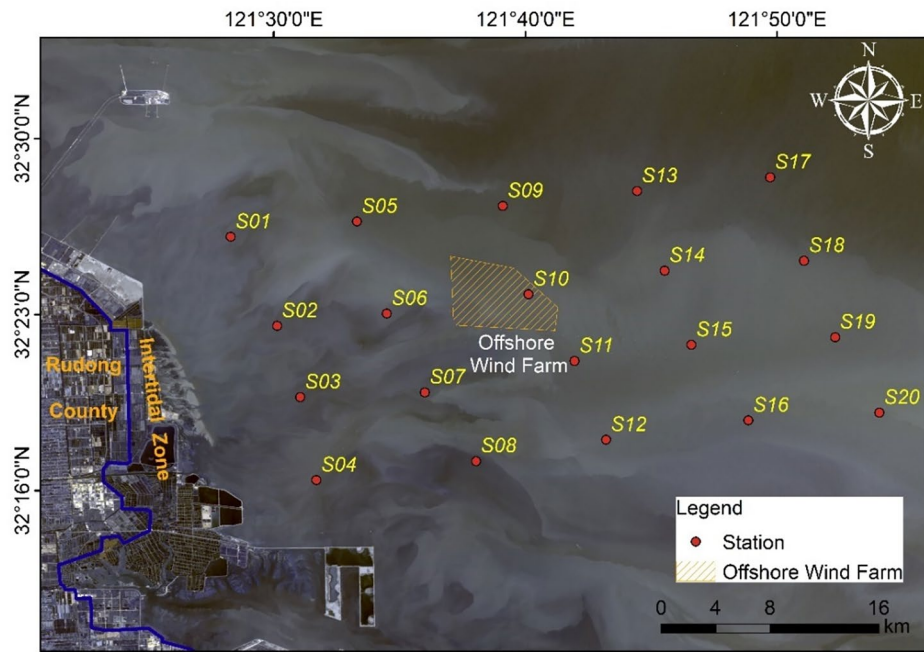


**Fig. 1.** Distribution of offshore wind farm and stations. The map is created using ArcGIS (Version 10.8), and the background satellite imagery is sourced from Landsat 8. (<https://www.gscloud.cn/sources/accessdata/411?pid=263>).

cases with numerous evaluation indicators. This method is relatively straightforward and ensures systematic and comprehensive evaluation results with good hierarchical structure. This study primarily conducts seawater quality assessments based on mathematical models of the index method.

- (1) Single-factor pollution index (P) and comprehensive water quality index (WQI)

$$P_{ij} = C_{ij}/S_i \tag{1}$$

$$WQI = \frac{1}{n} \sum_{i=1}^n P_{ij} \tag{2}$$

In which,  $P_{ij}$  represents the single-factor pollution index of the  $i$ th pollutant at the  $j$ th monitoring site;  $C_{ij}$  denotes the measured concentration of the  $i$ th pollutant at the  $j$ th monitoring site (mg/L);  $S_i$  indicates the threshold of environmental quality standard for the  $i$ th pollutant, with reference to the Class I standard in the "Water Quality Standards for Seawater" of China (GB3097—1997);  $WQI$  stands for the comprehensive water quality index;  $n$  represents the number of all evaluation indicators<sup>19</sup>.

The standard threshold values for each indicator are presented in Table 1. The assessment grades adhere to the pollution classification standards proposed by Luo et al. (Table 2)<sup>28</sup>.

- (2) Eutrophication Index (EI)

$$EI = \frac{COD \times TIN \times PH}{4500} \tag{3}$$

In which, EI represents the eutrophication index,  $COD$ ,  $TIN$  and  $PH$  is the measured concentration of chemical oxygen demand (mg/L), total inorganic nitrogen (mg/L), and phosphate (mg/L), respectively<sup>26</sup>.

The evaluation criteria are shown in Table 3.

- (3) Heavy Metal Pollution Index (HPI)

$$P_i = \frac{C_i}{S_i} \tag{4}$$

$$P_n = \sqrt{\frac{\max(P_i)^2 + \text{ave}(P_i)^2}{2}} \tag{5}$$

In which,  $P_i$  represents the single-factor pollution index,  $C_i$  denotes the measured concentration of heavy metal  $i$  (mg/L), and  $S_i$  indicates the corresponding standard threshold value (mg/L), referencing the Class I standard of the "Water Quality Standard for Seawater" (GB3097-1997) in China.  $P_n$  is the integrated heavy-metal pollution index (HPI),  $\max(P_i)$  and  $\text{ave}(P_i)$  denotes the maximum value and average value of single-factor pollution index for heavy metals, respectively<sup>27</sup>.

The evaluation standards for heavy metal pollution are presented in Table 4.

Indicator	Class 1 standard threshold	Reference standard
COD	2	“Water Quality Standards for Seawater” in China (GB3097—1997)
TIN	0.2	
PH	0.015	
PET	0.05	
Cu	0.005	
Pb	0.001	
Zn	0.02	
Cd	0.001	
Hg	0.00005	
As	0.02	

**Table 1.** Seawater quality standards (unit: mg/L).

WQI	Pollution level	Evaluation grade
$WQI < 0.75$	1	Clean
$0.75 \leq WQI < 1$	2	Slightly polluted
$1 \leq WQI < 1.25$	3	Moderately polluted
$WQI \geq 1.25$	4	Severely polluted

**Table 2.** Classification of WQI evaluation levels.

EI	Pollution level	Evaluation grade
$EI < 1$	1	Oligotrophic
$1 \leq EI < 3$	2	Mild eutrophication
$3 \leq EI < 9$	3	Moderate eutrophication
$EI \geq 9$	4	Severe eutrophication

**Table 3.** Classification of EI evaluation levels.

Spatial interpolation has become one of the important methods for gridding discrete site data<sup>27</sup>. The paper uses radial basis function interpolation in the ARCGIS spatial analysis module to derive continuous spatial distributions of pollution indices from data collected at 20 monitoring stations. This visualization aids in analyzing the spatiotemporal characteristics of marine water quality more intuitively. Furthermore, there may be differences in pollution sources and mechanisms of pollutant distribution and diffusion in different scenarios. This study distinguishes three different scenarios to compare and analyze the water environmental effects of OWF. Among them, S0 represents the baseline scenario, belonging to the pre-construction period, which represents the environmental background state without human intervention of OWF construction. S1 represents the construction period scenario, representing the environmental impact status dominated by the construction of OWF. S2 represents the operational period scenario, representing the environmental impact status dominated by the operation and management activities of OWF in the study area.

## Results and analysis

### Variation characteristics of single-factor pollution levels in seawater

Figure 2 compares the content characteristics of various single-factor pollutants in the surface seawater during different periods. In S1, compared to S0, the mean concentration of PET, TIN, PH ( $P \leq 0.01$ ), Pb, Cd ( $P \leq 0.001$ ),

$P_i$	$P_n$	Evaluation grade
$\leq 1$	$\leq 0.7$	Safe
1–2	0.7–1.0	Caution
2–3	1.0–2.0	Mild pollution
$> 3$	$> 2$	Severe pollution

**Table 4.** Assessment standards for seawater heavy metal pollution.

and Hg ( $p \leq 0.05$ ) increased, while COD ( $p \leq 0.05$ ), Cu ( $p \leq 0.05$ ), Zn ( $P \leq 0.001$ ) and As ( $p \leq 0.001$ ) decreased (Table 5). Compared to S1, the mean concentration of COD, TIN, Pb, Zn ( $P \leq 0.001$ ), and As ( $P \leq 0.001$ ) in S2 increased, while PET, PH, Cu, Cd, and Hg all decreased statistically significant ( $P \leq 0.001$ ) (Table 5). Compared to S0, the mean concentration of TIN, Pb, Cd, and Zn ( $P \leq 0.01$ ) in S2 increased, while PET ( $P \leq 0.001$ ), COD, PH ( $p \leq 0.05$ ), Cu ( $P \leq 0.001$ ), Hg, and As decreased (Table 5). Cu was the only parameter that showed a continuous decrease in concentration. Most indicators increased during the construction phase and then return to baseline levels or even lower during the operational phase, with the exception of Zn.

The above results suggest preliminarily that during the construction phase of the OWE, there was a high likelihood of exacerbating the rise in PET concentration, TIN pollution, PH pollution, localized heavy-metal Pb contamination, and elevated Cd and Hg concentrations. On the other hand, there was a possibility of benefiting the concentration decrease in COD, Cu, Zn, and As. During the operational phase, it might lead to an

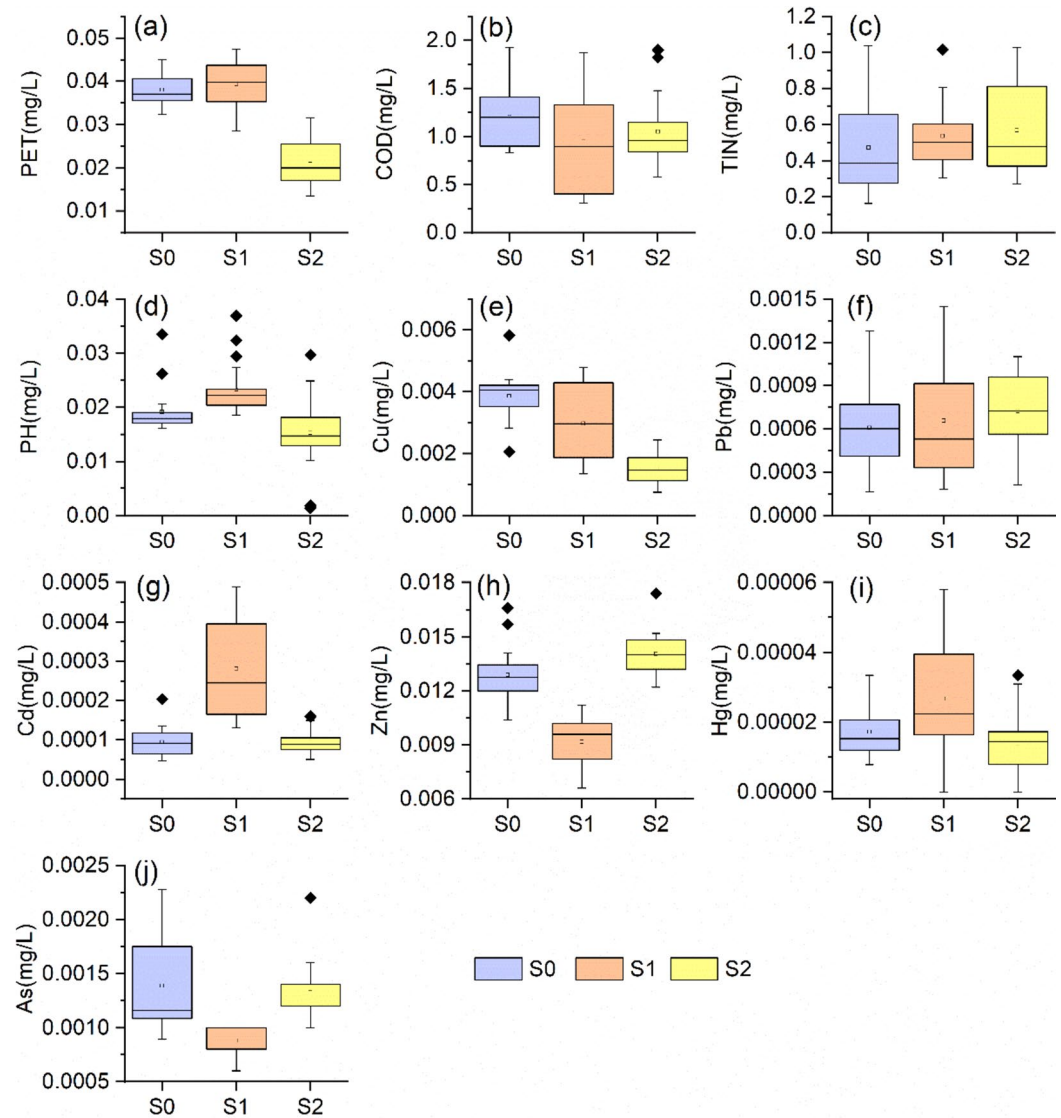


**Fig. 2.** Statistical characteristics of indicator concentrations at different stages.

Contrast	PET	COD	TIN	PH	Cu	Pb	Cd	Zn	Hg	As
S0:S1	- 1.15	2.67*	- 0.9	- 3.33**	2.72*	- 0.46	- 6.89***	7.44***	- 2.29*	5.21***
S1:S2	11.94***	- 0.68	- 0.39	4.07***	4.91***	- 0.51	6.47***	- 10.88***	3.74***	- 6.96***
S0:S2	11.53***	1.39	- 1.19	2.3*	10.42***	- 1.34	- 0.01	- 2.85**	1.15	0.49

**Table 5.** *t*-test for single-factor pollution index between different stages. The asterisk indicates the significance level, \*\*\* $P \leq 0.001$ , \*\* $P \leq 0.01$ , \* $P \leq 0.05$ .

exacerbation of TIN pollution and an increase in Zn concentration, while favoring the mitigation of PH pollution and the concentration decrease in PET, Cu, and Cd.

The single-factor pollution index further reveals the concentration levels of various pollutants (Fig. 3). Across stages S0 to S2, the surface water concentrations of PET, COD, Cu, Cd, Zn, Hg, and As at all sites were lower than the first-class standards set by "Seawater Quality Standard" (GB3097-1997). However, the concentrations of PH at all sites and almost all sites' concentrations of TIN exceeded the first-class standard (with most TIN levels exceeding the fourth-class standard). Additionally, the Pb concentrations at some sites exceeded the first-class standard (with 2, 4, and 5 sites exceeding the standard in S0, S1, and S2, respectively). Thus, the baseline values for PH and TIN concentrations in the study area were significantly elevated. In S0 (Fig. 3), the main pollutants in surface water were TIN (19 sites), pH (20 sites), Cu (1 site), and Pb (2 sites). In S1, they were TIN (20 sites), PH (20 sites), Pb (4 sites), and Hg (3 sites). In S2, they were TIN (20 sites), PH (9 sites), and Pb (5 sites).

Comparing different stages, the decrease in PET and Cu concentrations in S2 compared to S0 and S1 was more pronounced at most sites. Compared to S0, the decrease in COD in S1 mainly occurred at sites S1, S3, S9, S14, and S16–S17. There were significant differences in the increase in TIN concentrations between S1 and S0. For PH and Cd, compared to S0, most sites showed a general increase in concentrations in S1, but then decreased to S0 levels in S2. The Pb pollution in S1 compared to S0 mainly occurred at sites S6–S9, S11, S15, and S18;

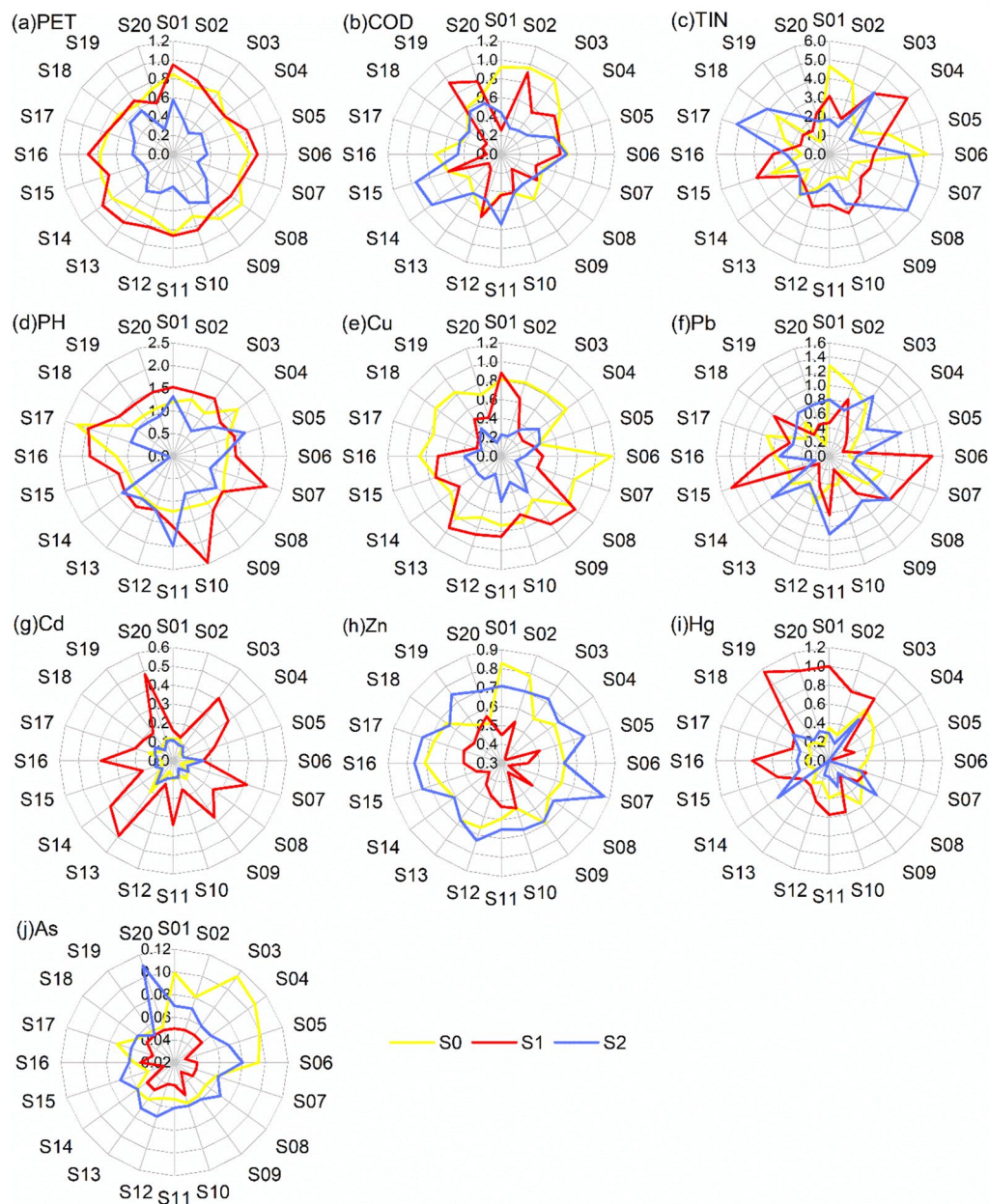


**Fig. 3.** Single-factor pollution index at different stages for each site.

compared to S0, the increase in concentration in S2 mainly occurred at sites S5, S8–S11, S13–S14, and S19–S20. For Zn, the concentrations at most sites significantly decreased in S1 compared to S0, while they significantly rebounded in S2 compared to S1, with the most significant increases observed at sites S5, S7, and S19–S20. The increase in Hg concentration in S1 compared to S0 was most pronounced at sites S1–S3, S15–S16, and S19–S20. For As, the most pronounced decrease in concentration relative to S0 occurred at sites S1–S7. In summary, the OWF's effects on PET, PH, Cd, Cu, and Zn exhibited good consistency among sites across different stages, while other factors showed significant differences among sites at each stage.

### Characteristics of water eutrophication

The EI elucidates the degree of eutrophication in seawater around OWF. The mean values of EI from the 20 sites indicate that S0, S1, and S2 had mean values of 2.62, 2.59, and 1.92, respectively, all indicating mild eutrophication (Table 3). However, there was a decreasing trend in EI, particularly during the operational phase, where the index showed the most significant decrease (see Table 6). The fluctuation range of EI among the 20 sites in S2 was 0.17–4.23 mg/L, much smaller than that of S0 and S1. These results suggest that there was a baseline mild eutrophication phenomenon in the study area, and the construction phase of OWF did not significantly exacerbate water eutrophication in general. Conversely, the operational phase helped alleviate the degree of water eutrophication to some extent. Combined with the analysis in the previous sections, this was primarily achieved by reducing COD and PH concentrations to mitigate moderate eutrophication.

The results from spatial interpolation based on EI values reveal significant differences in the spatial patterns of water eutrophication at different stages (Fig. 4). Prior to the construction of the OWF, moderate eutrophication in the study area was primarily concentrated in the western coastal regions, exhibiting an overall spatial pattern of moderate, mild, and oligotrophic eutrophication from northwest to southeast. During S1, moderate eutrophication remained concentrated in the western coastal areas but with a reduced extent (Table 6), accompanied by a shift in spatial morphology. From southwest to northeast, there was an overall transition from moderate to mild and oligotrophic eutrophication. In S2, the spatial pattern transformed again, gradually transitioning from moderate eutrophication around the OWF to mild and oligotrophic eutrophication in the outer periphery. The extent of moderate eutrophication significantly decreased (Table 6). Comparing the three stages, the most pronounced reduction in EI occurred in areas near the coastline, suggesting a potential correlation with the socioeconomic placement of the OWF.

### Assessment of heavy metal pollution

Comparing the average single-factor pollution indices from S0 to S2, Zn, Pb, and Cd generally rose in surface seawater, while Cu generally fell (Fig. 3). From the perspective of the HPI evaluation, the mean values of  $P_n$  in S0, S1, and S2 at 20 stations were 0.664, 0.705, and 0.634, respectively. Overall, there is a trend of initially increasing and then decreasing, with the evaluation level of heavy metal risk changing from safe to caution and then returning to safe. This can also be verified by the changes in the proportion of stations and area in Table 6. These results indicate that the background heavy metal content in the study area was relatively low, but the heavy metal pollution level increased during the construction period, mainly through the increase in Pb, Cd, and Hg concentrations.

From the perspective of spatial distribution (Fig. 5), prior to the construction of the OWF, the high concentration zones of heavy metals in the study area were primarily located in the northwest region near the coastal area, decreasing from northwest to southeast. This distribution pattern was broadly similar to that of water

Stage	Oligotrophic		Mild eutrophication		Moderate eutrophication		Severe eutrophication	
	Site	Area	Site	Area	Site	Area	Site	Area
EI								
S0	20%	3.3%	45%	67.1%	35%	29.6%	0	0
S1	20%	6.5%	40%	66.7%	40%	26.8%	0	0
S2	20%	13.9%	55%	79.3%	25%	6.9%	0	0
Stage	Safe		Caution		Mild pollution		Severe pollution	
	Site	Area	Site	Area	Site	Area	Site	Area
HPI								
S0	75%	74.7%	25%	25.3%	0	0	0	0
S1	45%	53.7%	45%	41.4%	10%	4.9%	0	0
S2	70%	81.4%	30%	18.6%	0	0	0	0
Stage	Clean		Slight pollution		Moderate pollution		Severe pollution	
	Site	Area	Site	Area	Site	Area	Site	Area
WQI								
S0	50%	57.1%	35%	34.8%	15%	8%	0	0
S1	30%	22.6%	65%	77.2%	5%	0.2%	0	0
S2	65%	80.2%	35%	19.8%	0	0	0	0

**Table 6.** Proportion of stations and area with different evaluation results.

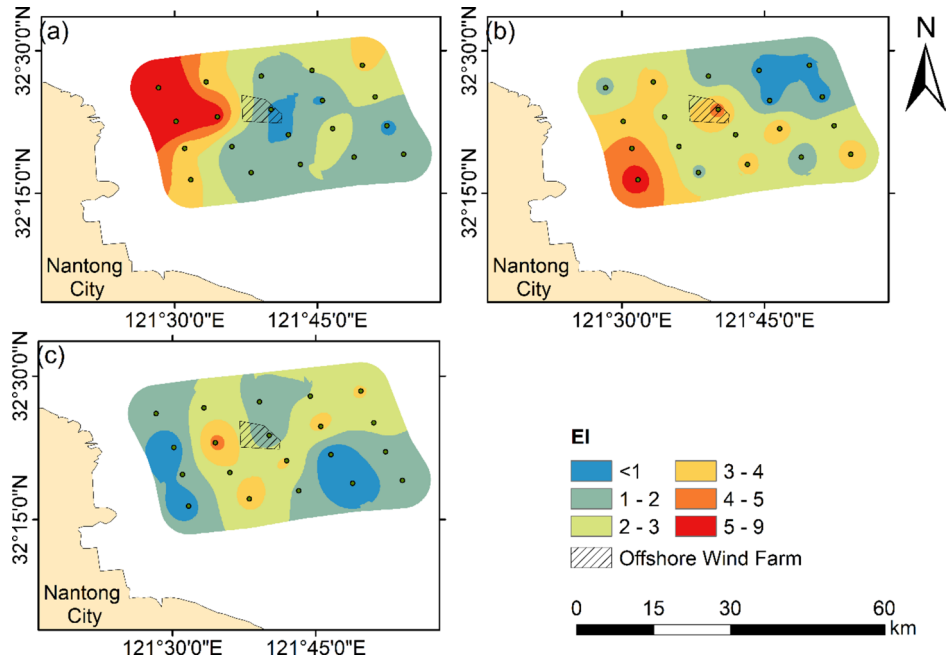


**Fig. 4.** Spatial patterns of seawater eutrophication index at different stages (a: S0, b: S1, c: S2).

eutrophication, indicating a significant influence of land on seawater quality. During S1, areas of mild heavy metal pollution were mainly distributed on both sides of the project area, with the left side exhibiting more severe pollution. Overall, there was an increase in heavy metal concentrations, with the areas of caution and mild pollution accounting for approximately 47% of the study area (Table 6). A shift in spatial morphology occurred. In S2, the spatial pattern transformed again, with the relatively high-value zones around the OWF gradually transitioning to lower-value areas outward. The areas of mild pollution disappeared, and the range of caution levels decreased, expanding the safety level coverage to 81.4% (Table 6). This indicates that during the operational period, the risk of heavy metal pollution from the OWF was relatively low and might contribute to alleviating coastal seawater heavy metal pollution. However, attention should be paid to the heavy metal pollution brought by the construction period in the surrounding areas of the OWF.

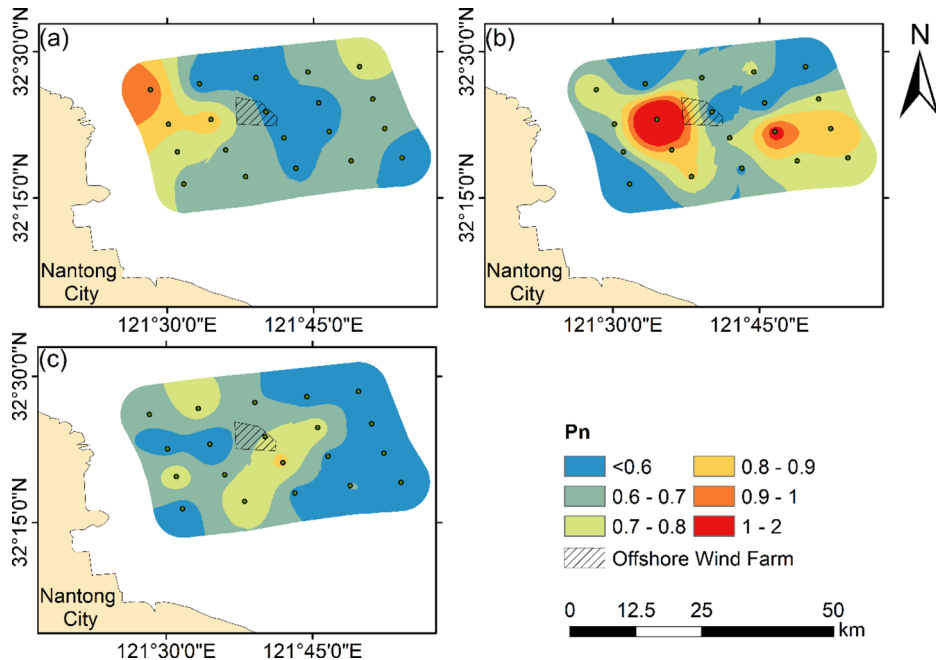


**Fig. 5.** Spatial patterns of heavy metal pollution index in seawater at different stages (a: S0, b: S1, c: S2).



### Comprehensive pollution assessment

The WQI index is a popular tool that aids in revealing the comprehensive pollution status of various types of pollutants. Statistics indicate that the average WQI values for S0, S1, and S2 across 20 stations were 0.754, 0.806, and 0.697, respectively. During S0 and S1, the overall seawater quality was characterized by mild pollution, whereas it reached a clean level in S2. The predominant pollutants contributing to seawater quality in S0 were ranked as follows: TIN > PH > Cu > PET > Zn > COD > Pb. In S1, the ranking shifted to TIN > PH > PET > Pb > Cu > Hg > COD. Meanwhile, in S2, the ranking was TIN > PH > Pb > Zn > COD > PET > Cu. Thus, it is evident that the primary pollutants in the surface seawater of the study area were TIN and PH, with slight variations in the influence of PET, Cu, Pb, Zn, and COD across different stages. Compared to the 50% in S0, the proportion of stations classified as clean had risen significantly to 65%, whereas those of mild level had fallen to 35% from 65% in S1, with no instances of moderate pollution or higher (Table 6).

From the spatial pattern depicted in Fig. 6, in S0, the WQI exhibited a spatial pattern of decreasing intensity from northwest to southeast, with pollution primarily concentrated near the northwest coastal areas. During S1, the WQI shifted to a decreasing trend from southwest to northeast, aligning closely with the pattern of EI. However, the extent of mild pollution significantly expanded, reaching 77.2%, an increase of 42.4% compared to S0 (Table 6). In S2, the spatial pattern of the WQI transformed as the mild pollution area on the southwest side of the OWF gradually transitioned towards cleaner areas on the periphery, resulting in an overall reduction in spatial heterogeneity (Fig. 6c). The area classified as clean expanded to 80.2% (Table 6). These findings indicate that from pre-construction to the construction phase, the areas classified as clean, mild pollution, and moderate pollution decreased by 34.5%, increased by 42.4%, and decreased by 7.8%, respectively. From pre-construction to the operational phase, the areas classified as clean, mild pollution, and moderate pollution increased by 23.1%, decreased by 15%, and decreased by 8%, respectively. The operation of the OWF contributed to the overall improvement of seawater quality in the region, particularly in mitigating the previously observed high pollution levels in the northwest coastal areas of the study area.

### Discussion

#### Mechanisms of pollution formation and diffusion at different phases of OWF

In contrast to many studies relying on qualitative analysis of OWFs, this study utilizes GIS and mathematical models to quantitatively assess the marine water quality impact of OWF along the Jiangsu coast across different scenarios. This aligns with the research approach advocated by prior studies, which employed a Before-After/Control-Impact methodology across the three life stages of OWFs to gain insights into their impact on the marine environment<sup>15,29</sup>. The findings reveal significant differences in the impact on marine water quality environment under different scenarios, whether in terms of individual pollutant concentrations or composite pollution indices. Overall, the adverse effects of OWF on the seawater environment primarily occurred instantaneously during the construction phase. Previous studies have similarly identified a pattern of wind farms having greater impacts on organisms during construction than subsequent operation<sup>7</sup>. However, the impact of wind farms during the operational phase remains highly controversial. In contrast to the prevailing belief that adverse effects would gradually diminish or revert to baseline levels post-construction<sup>15–17</sup>, the present study further reveals that operational OWF can contribute to a slight enhancement of seawater quality above baseline conditions.

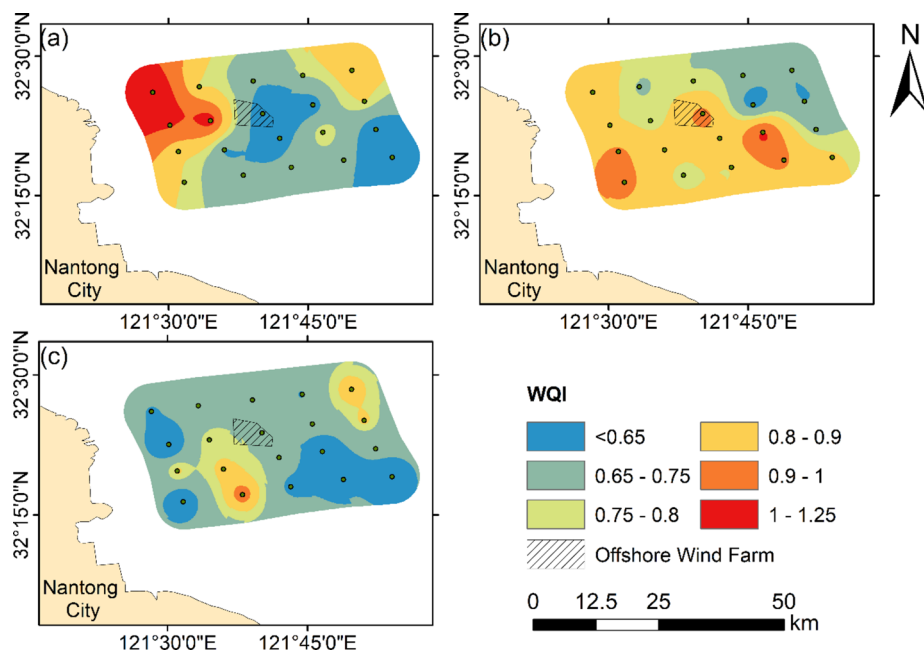


**Fig. 6.** Spatial pattern of comprehensive pollution indices in seawater during different stages (a: S0, b: S1, c: S2).

In terms of the sources and diffusion mechanisms of pollutants, various pathways during the construction phase may lead to water pollution<sup>8,10</sup>. The concentrations of PET, TIN, PH, Cd, and Hg were highest or elevated during the construction phase. This was because activities during OWF construction might lead to increased input of petroleum substances and nutrients (such as nitrogen and phosphorus) into the seawater, while also potentially releasing heavy metals such as Cd and Hg<sup>15,16</sup>. The increase in concentrations of Pb, Cd and Hg was the main reason for the significant increase in the comprehensive pollution risk of heavy metals during the construction phase. The concentrations of Zn and Pb were highest during the operational phase, likely related with normal operation and maintenance of wind power equipment. After OWF was operational, Zn was released into the water from galvanic anodes<sup>24</sup>. Gomiero et al. found the galvanic anodes as a source for Zn and Cd emission and accumulation in the mussels from an offshore gas platform in Adriatic Sea<sup>30</sup>. Other studies found that dissolved Zn initially increased and then gradually decreased through sorption by particulate matters and water dilution process<sup>31</sup>. Additionally, Zn and Pb were commonly used in corrosion protection and coating materials, which could release into the seawater when these materials were eroded by wind or corroded by seawater<sup>24</sup>. It is estimated that an OWF can emit 2000 kg zinc per year if assume that it consists of 80 OWT monopiles and one offshore survival system<sup>23</sup>. The concentration of Cu decreased significantly over time, likely due to Cu pollution mainly originating from industrial emissions along the coastal areas and inputs from inland rivers<sup>32,33</sup>. Cu metal is relatively easy to precipitate in weak alkaline seawater environments. After the construction of OWF, enhanced control and governance of the surrounding environment might contribute to the alleviation of Cu pollution.

It is necessary to consider the environmental impact of OWF in the context of the existing pressures (i.e. maritime traffic, chemical pollution, aquaculture development, fishery). The overall baseline water quality condition in the studying area was mild pollution, with the highest concentrations of TIN and PH exceeding the environmental quality standard, closely related to the natural and social backgrounds of the marine area itself<sup>33</sup>. The study area is located in the northern part of the Yangtze River Delta, one of the most economically developed regions in China, which continuously brings pollution sources and substances to the surrounding marine areas<sup>34</sup>. Coastal areas have extensive intertidal zone and mudflat wetland ecosystems, playing important ecological service functions. Although this enables some purifying effect on pollution, in recent years, ecological landscapes have shown obvious fragmentation due to factors such as aquaculture, leading to a decline in ecological functions<sup>35</sup>. The marine areas near the study area have been planned for multiple function zones ranging from mudflat aquaculture to port area, wind energy exploration, navigation area, anchorage area, and fishing<sup>36</sup>. These factors may be the main reasons for the severe excessive concentrations of TIN and PH in the study area, leading to water eutrophication.

Conversely, during the construction and operational phases, the EI index of the seawater continued to decline. This seems to contradict the report that OWF structures can contribute in nutrient concentration and primary production through a localized vertical mixing<sup>21</sup>. In the case study of the southwest Baltic Sea, Janßen et al. found that OWF structures could facilitate buildup of biomass and potentially intensify eutrophication, especially in already rich in nutrients and semi-enclosed water bodies<sup>37</sup>. However, it is suggested that a site for OWF with sufficient water renewal could mitigate eutrophication problems<sup>37</sup>. The coastal waters of Jiangsu Province, an open sea area with strong tides and ocean currents, may play a significant role in mitigating water eutrophication near OWF. Study on the North Sea indicated that annual primary production rate could change  $\pm 10\%$  as the result of stratification and generated wind wakes by OWFs<sup>13</sup>. Wang et al. proposed that the Rudong OWF could influence the structure and energy flow of coastal ecosystems<sup>18</sup>. Following construction, coastal ecosystems tended to develop towards higher maturity with higher energy throughput, ecosystem activity, and recycling capability<sup>18</sup>. This led to increased primary production, biomass, and fish production, indicating a potential “reef effect”<sup>16</sup>. It might be conducive to the absorption of excessive nutrients. Another important reason was likely due to the increased control and governance intensity of the surrounding ecological environment and aquaculture after the planning and construction of OWF<sup>36</sup>. Because poor marine water environments may also cause pollution or erosion effects on wind power facilities.

Under different scenarios, the spatial patterns of seawater quality environments had undergone significant adjustments, and the influencing factors and mechanisms might be more complex. Before the construction of OWF, the concentrations of various pollutants generally showed a spatial pattern of decreasing from northwest to southeast, which might be related to three main factors. First, it was the influence of land-based pollution inputs in the western part of the study area. Second, it was related to the control of regional tidal flow and current systems. The study area is located in the southern part of the radiating sandbar sea area, with complex and changeable terrain, mainly controlled by the eastward advancing tidal waves of the East China Sea, and the tidal flow effect is significant<sup>25,38</sup>. The tidal flow mainly exhibits a reciprocating flow pattern, with the main flow direction consistent with the coastline or groove direction. The dominant flow direction during rising tide is NWW, and during falling tide, it is SEE. The maximum flow velocity in the area ranges from 1.02 to 1.32 m/s, with the flow velocity decreasing with increasing water depth<sup>25</sup>. The above tidal flow system controlled the migration and diffusion of pollutants. Third, it was related to the typical monsoon atmospheric environment of eastern China, influenced by southeast winds in summer and northwest winds in winter. The above tidal flow system is closely related to the monsoon circulation system controlling the area.

During the construction and operational phases, the spatial patterns of water quality environments evolved from high-value areas around the southwest or engineering areas to decreasing towards the northeast or periphery. This phenomenon might be associated with the hydrodynamics and climatic disturbance effects of wind turbine and bases, which could influence the oceanic flow system or atmospheric circulation<sup>11,15</sup>. In areas with widespread deployment of wind farms, wind energy is efficiently converted into electricity through wind turbine blades. This can distort energy flow and circulation. For instance, wind farms can result in wind distortion over a radius of 5–20 km<sup>11</sup>. In some case, wind wakes caused by OWF can extend downwind of wind-farm arrays by 60 km or more<sup>14</sup>. A decrease in wind speed may weaken the ocean–atmosphere interaction. This on the one

hand reduces the accumulation of pollutants downwind, and on the other hand may lead to a weakening vertical mixing, thereby reducing the water eutrophication downwind. Recent result based on ocean-atmospheric numerical models implies that wind speed changes are found to reduce upwelling on the inshore side of OWFs and increase upwelling on the offshore side<sup>13</sup>. This may help explain why pollutants begin to accumulate on both sides of the OWF perpendicular to the prevailing wind direction (Fig. 4c, 5c and 6c). However, further research and validation are needed on the mechanisms mentioned above.

### Implication and limitation

The current findings highlight the necessity for regulated construction processes in OWF development, particularly targeting pollutants like excessive TIN, PH, and Pb at their sources. Additionally, emphasis should be placed on Zn's impact on seawater quality, necessitating mitigation measures during OWF operation. Optimizing spatial allocation and layout in harmony with regional environmental features, alongside pre-emptive environmental effect simulations, can mitigate adverse water impacts during construction and operation. Concurrent environmental monitoring and protection measures undertaken by either government or enterprises in the surrounding region during the development of OWFs will aid in pollution control. If OWFs' potential to reduce eutrophication can be validated in mechanism, integrating them with marine aquaculture, fostering locally adapted species, becomes vital<sup>39,40</sup>. This synergy can amplify benefits across aquaculture, seawater quality enhancement, and OWF development for the Jiangsu Coast.

The present study, limited to ten representative seawater quality indicators, may compromise the comprehensiveness of its evaluation. Given the seasonal fluctuations in seawater quality and the study's focus on spatial patterns and water quality comparisons across OWF development stages based solely on autumn samples, it lacks representation for capturing long-term, continuous changes. Future endeavors can incorporate longer-term observations to enhance seasonal comparisons, which is crucial for assessing the long-term impact of OWF operations on seawater quality. Moreover, the intricate OWF-ocean-atmosphere interaction and its influence on pollutant transport and diffusion across spatiotemporal scales pose a formidable challenge, necessitating further quantitative research.

### Conclusion

This study assessed the impact of an OWF along the Jiangsu coast on marine water quality at different stages. Before construction, surface seawater quality was mildly polluted, mainly due to TIN, PH, Pb, and Cu. During construction, Ph, Cd, and Hg increased significantly, while PET, TIN, and Pb (locally) concentrations rose obviously, and COD, Cu, Zn, and As decreased significantly. The main pollutants were TIN, PH, Pb, and Hg. During operation compared to pre-construction period, concentrations of PET, PH, Cu, and Cd significantly decreased, while Zn concentrations significantly increased. Additionally, concentrations of TIN and Pb also showed an obvious increase. The main pollutants were found to be TIN, PH, and Pb.

Construction phase of the OWF did not worsen seawater eutrophication but increased heavy metal pollution, particularly Pb, Cd, and Hg contaminations. Conversely, operational phases alleviated eutrophication, mainly by reducing PH and COD concentrations. Comprehensive pollution levels increased during construction but remained mild overall, similar to the pre-construction phase. However, water quality improved to a clear level during operation. Spatially, the spatial patterns of various pollution types varied significantly across different stages. Before the OWF construction, the spatial patterns of EI, HPI and WQI generally showed a decreasing trend from northwest to southeast, with pollution concentrated mainly in coastal areas near the northwest. During the construction phase, it evolved into a gradual decrease from high-value areas near the southwest or around the construction area towards the northeast, accompanied by intensified pollution and a significant expansion of the polluted area. In the operational phase, the spatial patterns of various indices shifted towards a decrease from high-value areas near the southwest or around the wind farm towards the periphery, with a general reduction in spatial heterogeneity and a notable expansion of the area with clean water quality. The changes in pollutant concentrations and spatial evolution characteristics mentioned above may be closely related to comprehensive effects from factors such as oil spills, discharge of construction wastewater, release of pollutants from power generation equipment, land-based pollution, marine aquaculture, OWF-ocean-atmosphere interaction, and marine management and protection policy.

### Data availability

The data in this study can be obtained by contacting the author Wei, Zhudeng, weizhudeng@126.com.

Received: 7 June 2024; Accepted: 28 August 2024

Published online: 06 September 2024

### References

1. IEA. *World Energy Outlook 2021* (International Energy Agency, Paris, 2021).
2. IPCC. *Climate Change 2022: Mitigation of Climate Change. Contribution of Working Group III to the Sixth Assessment Report of the Intergovernmental Panel on Climate Change* (Cambridge University Press, Cambridge, 2022).
3. GWEC. *Global Wind Report 2023* (Global Wind Energy Council, Brussels, 2023).
4. Bosch, J., Staffell, I. & Hawkes, A. D. Temporally explicit and spatially resolved global offshore wind energy potentials. *Energy* **163**, 766–781 (2018).
5. Potisomporn, P. & Vogel, C. R. Spatial and temporal variability characteristics of offshore wind energy in the United Kingdom. *Wind Energy* **25**, 537–552 (2022).
6. Garthe, S. *et al.* Large-scale effects of offshore wind farms on seabirds of high conservation concern. *Sci. Rep.* **13**, 4779 (2023).

7. Pearce-Higgins, J. W., Stephen, L., Douse, A. & Langston, R. H. W. Greater impacts of wind farms on bird populations during construction than subsequent operation: Results of a multi-site and multi-species analysis. *J. Appl. Ecol.* **49**, 386–394 (2012).
8. Petersen, J. K. & Malm, T. Offshore windmill farms: Threats to or possibilities for the marine environment. *Ambio* **35**, 75–80 (2006).
9. Wang, L. *et al.* Ecological impacts of the expansion of offshore wind farms on trophic level species of marine food chain. *J. Environ. Sci-China* **36**, 226–244 (2024).
10. Watson, S. C. L. *et al.* The global impact of offshore wind farms on ecosystem services. *Ocean Coast. Manag.* **249**, 107023 (2024).
11. van Berkel, J. *et al.* The effects of offshore wind farms on hydrodynamics and implications for fishes. *Oceanography* **33**, 108–117 (2020).
12. Gao, P. Understanding watershed suspended sediment transport. *Prog. Phys. Geog.* **32**, 243–263 (2008).
13. Daewel, U., Akhtar, N., Christiansen, N. & Schrum, C. Offshore wind farms are projected to impact primary production and bottom water deoxygenation in the North Sea. *Commun. Earth Environ.* **3**, 292 (2022).
14. Ouro, P. *et al.* Environmental impacts from large-scale offshore renewable-energy deployment. *Environ. Res. Lett.* **19**, 063001 (2024).
15. Dai, K. *et al.* Environmental issues associated with wind energy - A review. *Renew. Energy* **75**, 911–921 (2015).
16. Rezaei, F., Contestabile, P., Vicinanza, D. & Azzellino, A. Towards understanding environmental and cumulative impacts of floating wind farms: Lessons learned from the fixed-bottom offshore wind farms. *Ocean Coast. Manag.* **243**, 106772 (2023).
17. Hong, Y. *et al.* Benign water quality and phytoplankton status during the operation of Guishan offshore wind farm in the Pearl River Estuary, China. *Reg. Stud. Mar. Sci.* **77**, 103637 (2024).
18. Wang, J., Zou, X., Yu, W., Zhang, D. & Wang, T. Effects of established offshore wind farms on energy flow of coastal ecosystems: A case study of the Rudong offshore wind farms in China. *Ocean Coast. Manag.* **171**, 111–118 (2019).
19. Uddin, M. G., Nash, S. & Olbert, A. I. A review of water quality index models and their use for assessing surface water quality. *Ecol. Indic.* **122**, 107218 (2021).
20. Guatu, L. F., Menegon, S., Depellegrin, D., Zuidema, C. & Yamu, C. Spatial and temporal analysis of cumulative environmental effects of offshore wind farms in the North Sea basin. *Sci. Rep.* **11**, 10125 (2021).
21. Cazenave, P. W., Torres, R. & Allen, J. I. Unstructured grid modelling of offshore wind farm impacts on seasonally stratified shelf seas. *Prog. Oceanogr.* **145**, 25–41 (2016).
22. Elliott, M. The role of the DPSIR approach and conceptual models in marine environmental management: An example for offshore wind power. *Mar. Pollut. Bull.* **44**, iii–vii (2002).
23. Kirchgeorg, T. *et al.* Emissions from corrosion protection systems of offshore wind farms: Evaluation of the potential impact on the marine environment. *Mar. Pollut. Bull.* **136**, 257–268 (2018).
24. Reese, A., Voigt, N., Zimmermann, T., Irrgeher, J. & Pröfrock, D. Characterization of alloying components in galvanic anodes as potential environmental tracers for heavy metal emissions from offshore wind structures. *Chemosphere* **257**, 127182 (2020).
25. Li, K., Zhang, W. & Wang, J. Numerical simulation of tidal currents and estimation of tidal energy in the coastal waters of Jiangsu. *Hydro Sci. Eng.* **13**, 111–117 (2017) ((In Chinese)).
26. Acua, C., Lvarez, X., Lorenzo, O., Cancela, N. & Acua-Alonso, C. Assessment of water quality in eutrophized water bodies through the application of indexes and toxicity. *Sci. Total Environ.* **728**, 138775 (2020).
27. Asim, M. & Rao, K. N. Assessment of heavy metal pollution in Yamuna River, Delhi-NCR, using heavy metal pollution index and GIS. *Environ. Monit. Assess.* **193**, 103 (2021).
28. Luo, X., Zhu, Y., Zhang, L. & Yang, J. Assessment method for the impact of intensive sea use on marine ecological environment. *Acta Ecol. Sin.* **34**, 182–189 (2014) ((In Chinese)).
29. Martínez, M. L. *et al.* A systemic view of potential environmental impacts of ocean energy production. *Renew. Sust. Energ. Rev.* **149**, 111332 (2021).
30. Gomiero, A. *et al.* Use of multiple cell and tissue-level biomarkers in mussels collected along two gas fields in the northern Adriatic Sea as a tool for long term environmental monitoring. *Mar. Pollut. Bull.* **93**, 228–244 (2015).
31. Deborde, J. *et al.* Impact of galvanic anode dissolution on metal trace element concentrations in marine waters. *Water Air Soil Pollut.* **226**, 423 (2015).
32. Fan, H. *et al.* Comprehensive evaluation of the ecological environment in the Yangtze River Estuary and its adjacent waters. *Acta Ecol. Sin.* **39**, 4660–4675 (2019) ((In Chinese)).
33. Zhang, Y., Zhou, M. & Liu, Y. Evaluation of water factors in coastal waters of Jiangsu Province. *Environ. Sci. Manag.* **43**(5), 171–175 (2018) ((In Chinese)).
34. Wang, T. *et al.* Microplastics in a wind farm area: A case study at the Rudong Offshore Wind Farm, Yellow Sea. *China. Mar. Pollut. Bull.* **128**, 466–474 (2018).
35. Li, L. *et al.* Effects of tidal flat reclamation on the stability of coastal wetland ecosystem services: A case study in Jiangsu Coast. *China. Ecol. Indic.* **145**, 109697 (2022).
36. DEEJP. The 14th Five-Year Plan for Marine Ecological Environment Protection in Jiangsu Province No.[2022]51 (2022).
37. Janßen, H., Schroeder, T., Zettler, M. L. & Pollehne, F. Offshore wind farms in the southwestern Baltic Sea: A model study of regional impacts on oxygen conditions. *J. Sea Res.* **95**, 248–257 (2015).
38. Zhang, Z. & Song, Z. Study on tidal current turbulence shear stress in the offshore waters of Jiangsu. *Oceanol. Limnol. Sin.* **46**, 995–1000 (2015) ((In Chinese)).
39. Maar, M. *et al.* Multi-use of offshore wind farms with low-trophic aquaculture can help achieve global sustainability goals. *Commun. Earth Environ.* **4**, 447 (2023).
40. Buck, B. H., Krause, G. & Rosenthal, H. Extensive open ocean aquaculture development within wind farms in Germany: The prospect of offshore co-management and legal constraints. *Ocean Coast. Manag.* **47**, 95–122 (2004).

## Acknowledgements

The authors appreciate the anonymous reviewers for their constructive comments and suggestions that have significantly improved the content and quality of this manuscript.

## Author contributions

Conceptualization, Z.W. and W.Y.; methodology, Z.W., M.W.; software, M.W., Y.G.; validation, Z.W. and M.W.; formal analysis, Z.W.; resources, A.J., Y.G., Z.Y. and Z.W.; writing—original draft preparation, Z.W.; writing—review and editing, Z.W. and W.Y.; revision—Z.W., W.Y., Z.Y. and Z.W.; visualization, M.W.; funding acquisition, W.Y. and Z.W. All authors have read and agreed to the published version of the manuscript.

## Funding

This study is under the auspices of the National Natural Science Foundation of China (U20A2098, 41701219) and the National Key Research and Development Program of China (“The Second Tibetan Plateau Scientific Expedition and Research Program (STEP)”, 2019QZKK0804).

### Competing interests

The authors declare no competing interests.

### Additional information

**Correspondence** and requests for materials should be addressed to Z.W. or W.Y.

**Reprints and permissions information** is available at [www.nature.com/reprints](http://www.nature.com/reprints).

**Publisher's note** Springer Nature remains neutral with regard to jurisdictional claims in published maps and institutional affiliations.

**Open Access** This article is licensed under a Creative Commons Attribution-NonCommercial-NoDerivatives 4.0 International License, which permits any non-commercial use, sharing, distribution and reproduction in any medium or format, as long as you give appropriate credit to the original author(s) and the source, provide a link to the Creative Commons licence, and indicate if you modified the licensed material. You do not have permission under this licence to share adapted material derived from this article or parts of it. The images or other third party material in this article are included in the article's Creative Commons licence, unless indicated otherwise in a credit line to the material. If material is not included in the article's Creative Commons licence and your intended use is not permitted by statutory regulation or exceeds the permitted use, you will need to obtain permission directly from the copyright holder. To view a copy of this licence, visit <http://creativecommons.org/licenses/by-nc-nd/4.0/>.

© The Author(s) 2024